JES Focus Issue on Lithium–Sulfur Batteries: Materials, Mechanisms, Modeling, and Applications

What Limits the Rate Capability of Li-S Batteries during Discharge: Charge Transfer or Mass Transfer?

T. Zhang,[a,z] M. Marinescu,[a] S. Walus,[b] P. Kovacik,[b] and G. J. Offer[a]

[a]*Department of Mechanical Engineering, Imperial College London, SW7 2AZ, United Kingdom*
[b]*OXIS Energy Ltd, E1 Culham Science Centre, Abingdon OX14 3DB, United Kingdom*

Li-S batteries exhibit poor rate capability under lean electrolyte conditions required for achieving high practical energy densities. In this contribution, we argue that the rate capability of commercially-viable Li-S batteries is mainly limited by mass transfer rather than charge transfer during discharge. We first present experimental evidence showing that the charge-transfer resistance of Li-S batteries and hence the cathode surface covered by Li_2S are proportional to the state-of-charge (SoC) and not to the current, directly contradicting previous theories. We further demonstrate that the observed Li-S behaviors for different discharge rates are qualitatively captured by a zero-dimensional Li-S model with transport-limited reaction currents. This is the first Li-S model to also reproduce the characteristic overshoot in voltage at the beginning of charge, suggesting its cause is the increase in charge transfer resistance brought by Li_2S precipitation.

Manuscript submitted May 11, 2017; revised manuscript received June 5, 2017. Published June 14, 2017. *This paper is part of the JES Focus Issue on Lithium-Sulfur Batteries: Materials, Mechanisms, Modeling, and Applications.*

Achieving a high practical energy density in Li-S batteries requires increased sulfur loading and reduced electrolyte loading at cell level. However, increasing the sulfur-to-electrolyte mass ratio lowers the sulfur utilization as well as the rate capability.[1–3] The charge rate of Li-S batteries is mainly limited by the large initial overpotential associated with the activation of precipitated Li_2S,[4] as well as the slow subsequent dissolution that could lead to incomplete Li_2S conversion at the end of charge.[5] The mechanisms behind the low discharge rate capability have been explained in terms of mass transport limitation and surface passivation caused by the accumulation of precipitated Li_2S.

The transport limitation could arise from high electrolyte viscosity and pore-blocking due to localized Li_2S precipitation. We recently demonstrated that a Li-S cell discharged at high current can provide extra capacity after an hour of relaxation.[6] With a one-dimensional Li-S model, it was found that slow ionic transport could force polysulfides to accumulate temporarily in the separator, leading to the known reduced capacity at high discharge rates. The capacity recovery phenomenon is the result of redistribution of polysulfides across the cell during relaxation. Danner et al.[7] further demonstrated with a multiscale Li-S model that localized precipitation tends to occur at the carbon-sulfur particle surface, leading to pore-blocking and transport-limited discharge capacity for high sulfur loading.

The insulating and insoluble discharge product, Li_2S, has been shown experimentally to cover active cathode surfaces during discharge and increase the charge-transfer resistance. The relation between discharge rate and morphology of the precipitate, however, remains under debate. Based on ex-situ SEM imaging of a carbon fiber ultramicroelectrode of a Li-S cell, Fan et al.[8] revealed that Li_2S formed as a thin, continuous coating after a fast discharge but appeared as a small number of large particles after a slow discharge. It was therefore hypothesized that the surface coverage by Li_2S, which is enhanced at larger polarizations, is the main limiting factor of the rate capability of Li-S cells. Lang et al.[9] demonstrated a different Li_2S morphology evolution behavior using in-situ AFM, where it was found that larger, lamellae structure of Li_2S were formed at high discharge rate whereas smaller nanoparticles of Li_2S_2 were formed during lower rate discharge. The experimental setup in both imaging studies, however, were not representative of a real Li-S battery that has much lower electrolyte-to-sulfur mass ratio. Based on the observations by Fan et al.,[8] Ren et al.[10] presented a Li_2S nucleation and growth model that assumes the Li_2S nucleation rate – and subsequently the rate of electrode surface coverage - increase with cathode overpotential. The Li-S model incorporating this nucleation and growth mechanism produced a good fit with experimental constant-current discharge curves at different rates. It also qualitatively captured the average Li_2S particle size after different discharge rates as observed with SEM. The model was not used to study the charging of Li-S cells.

In this study, we report new features in the charge/discharge behavior of a pouch Li-S cell that indicate mass transfer, rather than charge transfer, is the main factor limiting the discharge rate capability of Li-S batteries. We find that the capacity and resistance of a Li-S cell remain unchanged after a high-rate discharge. We also demonstrate the overpotential at the beginning of charge is determined by the capacity rather than the rate of the previous discharge. These observations contradict the hypothesis that Li_2S surface coverage is rate-dependent, and indicate that surface passivation - and the consequent increase in charge-transfer resistance - is not the main mechanism limiting the rate capability of practical Li-S batteries. Instead, we show that a simple Li-S model incorporating transport-limited reaction currents qualitatively captures the observed charge/discharge behavior.

Experimental

Experiments were performed on a Li-S pouch cell (OXIS Energy Ltd.) with a rated capacity of 10 Ah. Charge /discharge cycles were performed at 30°C with a Bio-Logic VMP3 potentiostat. Galvanostatic electrochemical impedance spectroscopy (GEIS) was performed on a single electrode pair Li-S pouch cell with a capacity of 200 mAh with a Bio-Logic VMP3 potentiostat at 30°C. The GEIS was measured at 16 mAh intervals during cell discharge at different rates, and a 1 hour rest was introduced between each discharge and GEIS measurement, in order to allow the cell to return to open-circuit potential. An alternating current of 10 mA with frequencies from 10 kHz to 1 Hz was applied. The measured impedance spectra were fitted with an equivalent circuit consists of resistors and constant-phase elements (Figure 3a) using Zview software following the method described by Kolosnitsyn et al.[11]

Results and Discussion

In the stepwise discharge experiment shown in Figure 1a, the cell was discharged at 0.2 C for 5 Ah and then at 1 C until reaching the voltage limit of 1.5 V, after which it was immediately discharged again

[z]E-mail: t.zhang@imperial.ac.uk

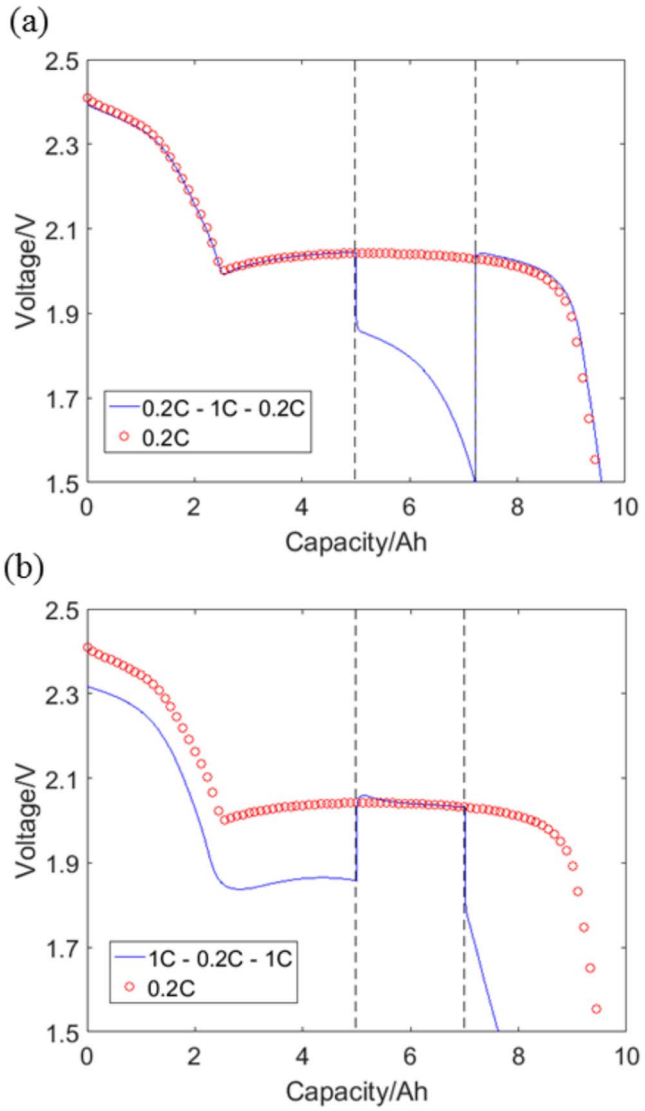

Figure 1. Discharge profiles at 0.2 C and at (a) 0.2 C-1 C-0.2 C steps, and (b) 1 C-0.2 C-1 C steps.

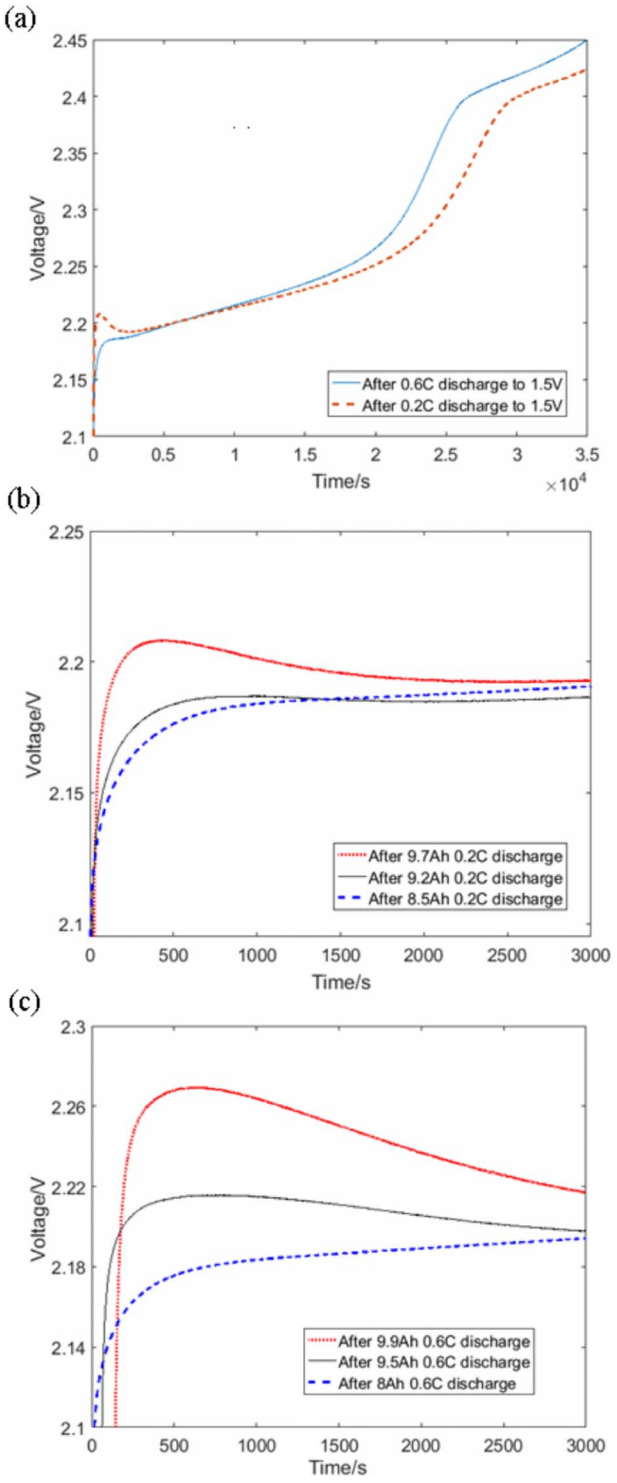

Figure 2. (a) Charge profiles at 0.1 C after 0.2 C and 0.6 C discharges to 1.5 V; (b) beginning of charge profiles at 0.1 C after 0.2 C discharge to different capacities; (c) beginning of charge profiles at 0.1 C after 0.6 C discharge to different capacities.

at 0.2 C. Surprisingly, not only was the cell able to discharge at 0.2 C instantly following the 1 C discharge, but also the total capacity of the 0.2 C-1 C-0.2 C discharge was the same as that of a constant-current 0.2 C discharge. Furthermore, the overlapping of the voltage curves in Figure 1a during the 0.2 C periods indicates the resistance and capacity of the cell were unaffected by the 1 C discharge period in-between. Similarly, there is an overlap between the voltage curves of the constant-current 0.2 C discharge and of the 0.2 C period of the 1 C-0.2 C-1 C stepwise discharge (Figure 1b). These observations contradict the rate-dependent Li_2S surface coverage theory proposed in Refs. 8,10 which would lead to an increase in cell resistance after the 1 C period due to increased Li_2S surface coverage. We assume the Li_2S morphology and its surface coverage cannot change instantaneously with current rate.

A small kink is often observed at the beginning of a Li-S charge curve as shown in Figure 2a. This kink represents a larger charge overpotential caused by the higher surface coverage by Li_2S at the beginning of charge/end of discharge.[11,12] If the Li_2S surface coverage were rate dependent, the charge overpotential would be larger after a high-rate discharge because of the higher Li_2S surface coverage at the end of the discharge. However, the opposite trend was observed in Figure 2a where the charge after a 0.6 C discharge to 1.5 V exhibits a lower initial overpotential than the charge after a 0.2 C discharge to 1.5 V. This trend was also observed by Poux et al.,[4] who explained the reduction in the charge overpotential as the consequence of reduced formation of Li_2S at the end of the higher rate discharge, that also exhibit lower discharge capacity. In agreement with Poux et al.'s explanation, we found that the charge overpotential is determined by the capacity instead of the rate of the previous discharge. Figure 2b

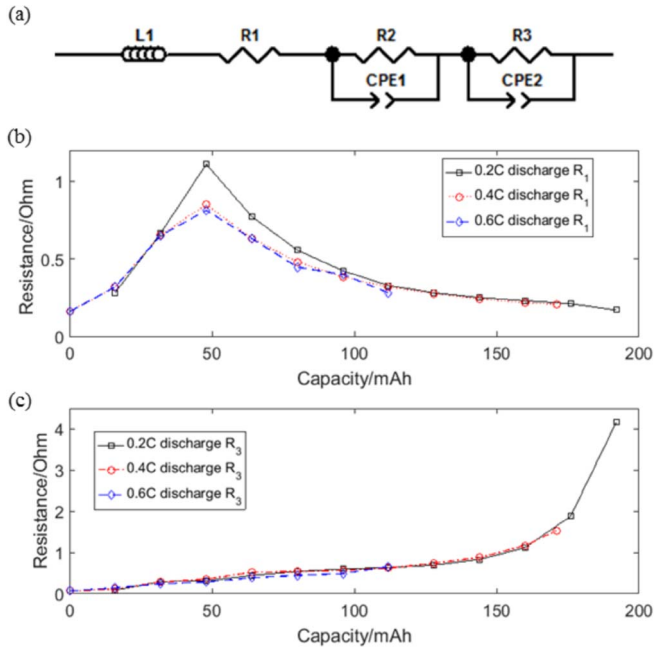

Figure 3. (a) Equivalent circuit network used to fit the GEIS measurements;[11] (b-c) the evolution of R_1 and R_3 during discharges at different rates.

indicates the charge overpotential after a 0.2 C discharge can be reduced by shortening the previous discharge. Similarly, Figure 2c shows the charge overpotential can be increased after a 0.6 C discharge if the discharge capacity is extended by lowering the voltage limit below 1.5 V. These observations on the initial charge overpotential confirm that the electrode surface coverage by Li_2S – the reason behind the initial charge kink – is not dependent on the current rate, but instead on the cell SoC.

Resistances measured by GEIS during discharge at different rates are compared in Figure 3. The high frequency resistance (R_1) is dominated by the resistance of electrolyte that varies with ionic concentration during discharge, but is unaffected by the current.[13] The low frequency resistance (R_3) is commonly interpreted as the resistance due to charge-transfer reactions in the cathode. R_3 increases during discharge due to increasing surface passivation by Li_2S.[11] The fact that R_3 appears to be the same at three different discharge rates at all SoCs again suggests Li_2S surface coverage is SoC-dependent but not current-dependent.

All preceding experiments indicate the surface coverage by Li_2S is not current-dependent, and consequently the rate capability of Li-S cells during discharge is not limited by surface passivation. The above charge/discharge behavior can be captured with a simple, zero-dimensional Li-S model with transport-limited reaction current densities. The model, introduced in Refs. 5,13, captures electrochemical reactions, precipitation and dissolution of Li_2S, as well as the dependence of cell potential and resistance on polysulfide concentrations. The model formulation and parameters are detailed in the supplementary materials. To include mass transfer limitation, we employ the following transport-limited form of Butler-Volmer equation to describe the reaction currents:[14]

$$\frac{I_j}{a_v V i_j} = \left(1 - \frac{I_j}{I^{lim}}\right) \exp\left(\frac{-F\eta_j}{2RT}\right) - \left(1 + \frac{I_j}{I^{lim}}\right) \exp\left(\frac{F\eta}{2RT}\right). \quad [1]$$

Here, I_j is the current of reaction j, i_j is the exchange current density of reaction j, a_v is the specific surface area of the cathode, V is the cell volume, η_j is the overpotential of reaction j, and I^{lim} is the limiting current due to mass transfer, assumed here to be the same for all reactions. The specific surface area in the porous electrode depends on the amount of Li_2S dissolved/precipitated during charge/discharge.

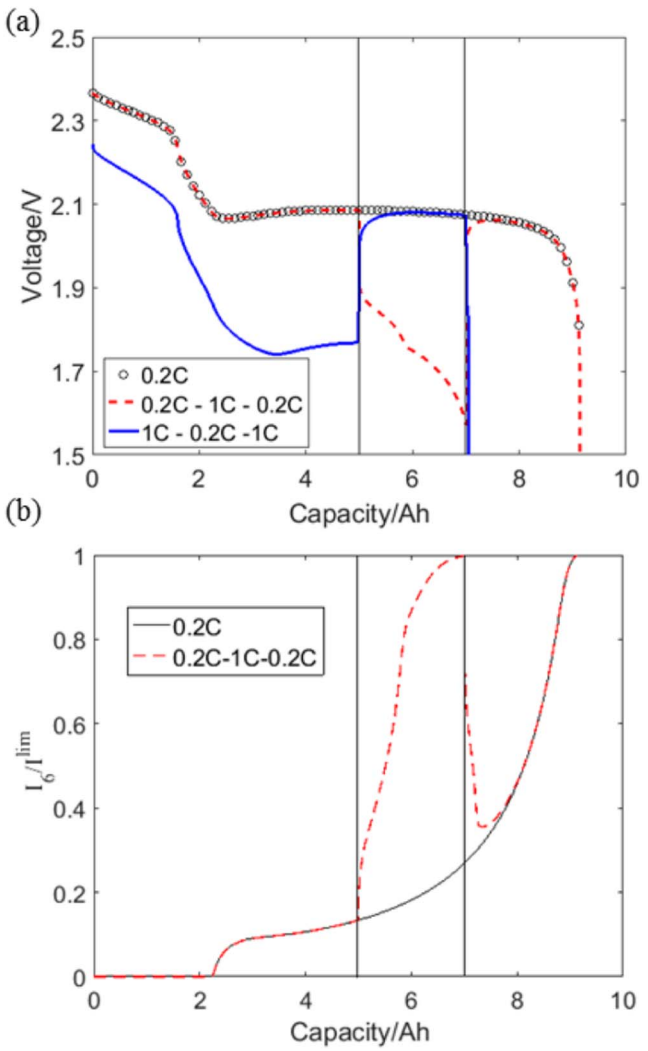

Figure 4. (a) Simulated discharge profiles at 0.2 C, 0.2 C-1 C-0.2 C steps, and 1 C-0.2 C-1 C steps; (b) simulated ratio between the reaction current for S_2^{2-} reduction, I_6, and the limiting current during discharges at 0.2 C and at 0.2 C-1 C-0.2 C steps.

This dependency is often modelled by a phenomenological expression of the following form Ref. 15:

$$a_v = a_{v,0}\left(1 - \frac{v_{Li_2S}}{v_{Li_2S,max}}\right)^{\theta_1}, \quad [2]$$

where $a_{v,0}$ is the initial specific surface area, v_{Li_2S} is the volume fraction of precipitated Li_2S, $v_{Li_2S,max}$ is the maximum volume fraction of Li_2S, and θ_1 is a fitting constant with a value of 0.5 in our simulations. The limiting current, I^{lim}, represents the maximum current carried by the diffusion of reactants toward the electrode surface and is dependent on the morphology and thickness of the Li_2S film covering the electrode. For simplicity, we assume I^{lim} is a function of the amount of Li_2S in a form similar to Eq. 2:

$$I^{lim} = I_0^{lim}\left(1 - \frac{v_{Li_2S}}{v_{Li_2S,max}}\right)^{\theta_2}, \quad [3]$$

where I_0^{lim} is the initial limiting current with no Li_2S and θ_2 is another fitting constant with an assumed value of 1.5.

As shown in Figure 4a, the Li-S model qualitatively captures the behavior of both 0.2 C-1 C-0.2 C and 1 C-0.2 C-1 C stepwise discharge experiments. During the 1 C period, the reaction currents are close to the limiting current ($I_j/I^{lim} \rightarrow 1$, as shown in Figure 4b for the

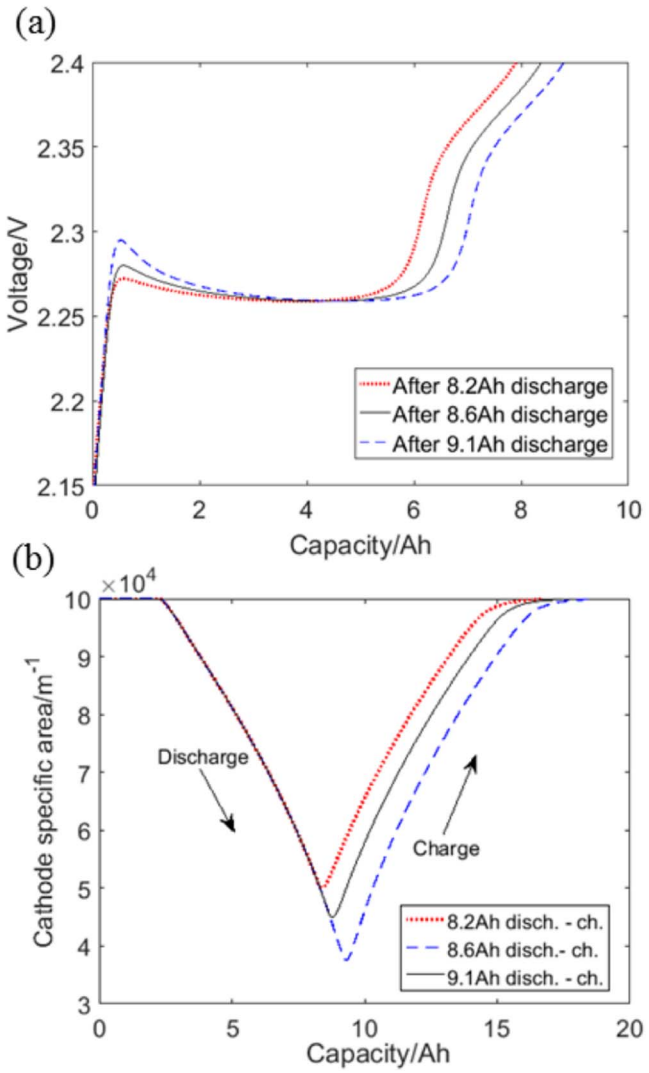

Figure 5. (a) simulated charge profiles at 0.1 C after 0.2 C discharge to various capacities, (b) the corresponding simulated available cathode specific area during the discharge-charge processes.

current corresponding to the reduction of S_2^{2-} into S^{2-}), leading to large overpotentials especially toward lower SoC where the limiting current is further reduced by the increasing amount of Li_2S that could impede ionic transport ($v_{Li_2S}/v_{Li_2S,max} \rightarrow 1$). Once the current is switched back to 0.2 C, the overpotential associated with mass transfer is instantaneously reduced ($I_j/I^{lim} < 1$) so the cell can be discharged further.

In Figure 5a, the model also qualitatively retrieves the trend of decreasing initial charge overpotential after the previous discharge leaves the cell in a higher SoC. The corresponding simulated cathode specific area is shown in Figure 5b for discharges and charges to different SoCs. Higher SoC translates to higher specific surface area available at the end of discharge due to reduced Li_2S formation ($v_{Li_2S} < v_{Li_2S,max}$), and therefore the charge transfer overpotential is smaller at the beginning of the subsequent charge. This is the first time this characteristic kink at the beginning of charge is captured by a Li-S model.

Conclusions

We present results that prove mass transfer, rather than charge transfer, is the limiting factor for the rate capability of a practical Li-S battery during discharge. By showing that a Li-S cell is able to discharge at 0.2 C immediately following a 1 C discharge without an increase in resistance, we conclude that electrode passivation by Li_2S does not significantly increase with current. These results indicate that the rate-dependent Li_2S surface coverage theory proposed in Refs. 8, 10 is not relevant to operation of real cells. We demonstrate that a simple Li-S model is able to capture the observed charge/discharge behavior by the addition of phenomenological expressions relating the Li_2S surface coverage and the transport-limited current to the quantity of Li_2S precipitated. The results should be of interest to materials developers, as they suggest results from experiments with high electrolyte-to-sulfur ratio, e.g. coin cells, may not be good indicators of performance in commercially viable cells where mass transfer will become limiting.

Acknowledgments

The authors thank the Engineering and Physical Sciences Research Council in the UK for funding this work under the Revolutionary Electric Vehicle Battery (REVB) project EP/L505298/1.

References

1. M. Hagen, D. Hanselmann, K. Ahlbrecht, R. Maça, D. Gerber, and J. Tübke, *Adv. Energy Mat.*, **5**, 1401986 (2015).
2. M. Hagen, P. Fanz, and J. Tübke, *J. of Power Sources*, **264**, 30 (2014).
3. J. Brückner, S. Thieme, H. T. Grossmann, S. Dörfler, H. Althues, and S. Kaskel, *J. Power Sources*, **268** 82 (2014).
4. T. Poux, P. Novák, and S. Trabesinger, *J. Electrochem. Soc.*, **163**, A1139 (2016).
5. M. Marinescu, T. Zhang, and G. J. Offer, *Phys. Chem. Chem. Phys.*, **18**, 584 (2016).
6. T. Zhang, M. Marinescu, S. Walus, and G. J. Offer, *Electrochimica Acta*, **219**, 502 (2016).
7. T. Danner, G. Zhu, A. F. Hofmann, and A. Latz, *Electrochimica Acta*, **184**, 124 (2015).
8. F. Y. Fan, W. C. Carter, and Y. -M. Chiang, *Adv. Mat.*, **27**, 5203 (2015).
9. S. -Y. Lang, Y. Shi, . Y. -G. Guo, D. Wang, R. Wen, and L. -J. Wan, *Angew. Chem. Int. Ed.*, **55**, 15835 (2016).
10. Y. X. Ren, T. S. Zhao, M. Liu, P. Tan, and Y. K. Zeng, *J. Power Sources*, **336**, 115 (2016).
11. V. S. Kolosnitsyn, E. V. Kuzmina, E. V. Karaseva, and S. E. Mochalov, *J. Power Sources*, **196**, 1478 (2011).
12. S. S. Zhang, *Energies*, **5**, 5190 (2012).
13. T. Zhang, M. Marinescu, L. O'Neill, M. Wild, and G. Offer, *Phys. Chem. Chem. Phys.*, **17**, 22581 (2015).
14. A. J. Bard and L. Faulkner, *Electrochemical Methods: Fundamentals and Applications*, John Wiley & Sons, New York, 2001.
15. K. Kumaresan, Y. Mikhaylik, and R. E. White, *J. Electrochem. Soc.*, **155**, A576 (2008).